Bulletin of Earthquake Engineering
https://doi.org/10.1007/s10518-021-01114-z

ORIGINAL ARTICLE

Seismic intensity measures for risk assessment of bridges

Gerard J. O'Reilly[1]

Received: 5 February 2021 / Accepted: 26 April 2021

Abstract
In performance-based seismic assessment, structural response is characterised using fragility functions based on a seismic intensity measure (IM). IMs are typically related to the characteristics of ground shaking and structural dynamic properties, with the spectral acceleration at the first and dominant mode of vibration, $Sa(T_1)$, being a popular choice for buildings. In bridge structures, where no single dominant mode typically exists for bridges with some degree of irregularity, the use of $Sa(T_1)$ may be inefficient (i.e. large dispersion) due to multi-modal transverse response. To avoid having to choose a single bridge mode when using $Sa(T_1)$ and to appease the needs of bridge portfolio assessment, peak ground acceleration (PGA) can often be the IM used for bridge fragility functions in some countries. This study examines the efficient assessment of simple bridge structures characteristic of the European context by exploring different IMs based on $Sa(T)$, peak ground velocity (PGV) or a recent candidate average spectral acceleration, *AvgSa*. Several case study bridges are evaluated via multiple stripe analysis with hazard-consistent ground motion records. The results indicate that PGA and PGV are indeed inefficient IMs compared to other IMs of similar complexity, especially at serviceability limit states, for the bridge structures examined. Also, a relatively casual record selection strategy is seen to not be suitable for risk assessment of bridges and can result in notable differences in risk. In contrast, *AvgSa*, which is an IM based on a simple combination of $Sa(T)$ values across a range of periods, showed very good predictive power and robustness in terms of its risk estimates across all ranges of structural response. This was observed for the structure-specific IMs in addition to the group IMs used for assessing multiple structures with the same ground motion records. This study has thus shown these *AvgSa*-based IMs to be an appealing choice to consider for further examination in future fragility function and risk model development for bridge structures.

Keywords PBEE · Risk · Fragility function · Intensity measure · Bridge

✉ Gerard J. O'Reilly
gerard.oreilly@iusspavia.it

[1] Centre for Training and Research on Reduction of Seismic Risk (ROSE Centre), Scuola Universitaria Superiore IUSS Pavia, Pavia, Italy

Published online: 05 May 2021

1 Introduction

Analysis and evaluation comprise key steps in risk assessment and management, where evaluation comprises using analysis outputs to make better and more informed decisions when aiming to manage and reduce risk. Thus, the quality of these analysis outputs is critical to good decision-making. In earthquake engineering, risk assessment typically involves analysing the performance of a structure or group of structures/infrastructures using what is broadly termed performance-based earthquake engineering (PBEE) (Cornell and Krawinkler 2000). Performance in this context may be generally described by the number of casualties, monetary losses (direct and indirect) and downtime caused by earthquake-induced shaking. It is the quantification of these that is the focus of risk assessment and management within the context of earthquake engineering.

With this objective in mind, engineers break down the problem of structural assessment in terms of distinct indicators, or limit states, which describe the performance of a structure, or group of structures, in quantifiable terms. Various approaches exist for structural typologies to quantify each of the three performance indicators. For example, the collapse capacity of a structure can be estimated using analysis procedures like incremental dynamic analysis to determine the distribution of seismic shaking intensities causing collapse and subsequently estimate casualties. Mackie et al. (2009) described a procedure to estimate expected monetary losses in bridges whilst also dealing with some of the more indirect consequences like expected downtime. Kilanitis and Sextos (2019) proposed a risk management framework to quantify the resilience of bridge networks via the distinct consideration of direct and indirect sources of loss. These methodologies seek to link the performance of structures to the level of ground shaking required to induce them.

If a structure's limit state capacity is denoted as C and the seismic demand denoted as D, being able to quantify the exceedance is what is of interest (i.e. when $D > C$). Given the uncertain nature of ground motion shaking in structures, D being greater than C cannot be stated with absolute certainty, hence the conditional probability of this exceedance is used. More formally, the probability of D exceeding C for a given intensity measure level (IML), s, is denoted $P[D > C|s]$. This can usually be characterised by a lognormal distribution described by a median, η, and dispersion, β, as shown in Fig. 1, and is termed a seismic fragility function, as discussed in Cornell et al. (2002). When integrated across all intensities of the mean hazard curve obtained from probabilistic seismic hazard analysis

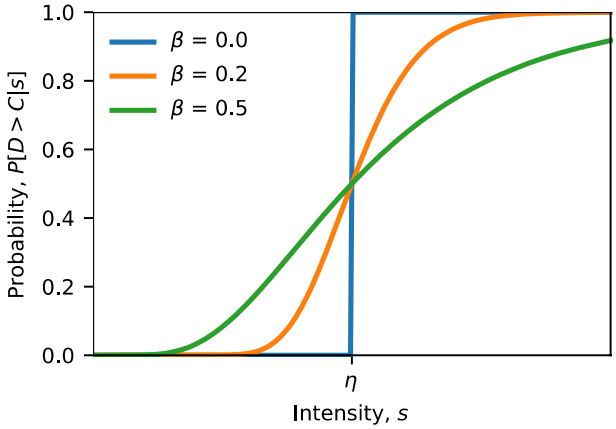

Fig. 1 Illustration of seismic fragility curves with the same median value, η, describing the conditional probability of the demand, D, exceeding the capacity, C, with respect to the seismic intensity, s, for increasing levels of dispersion (orange and green) and also no dispersion (blue)

(PSHA), $H(s)$, it gives the mean annual frequency of exceedance (MAFE) (Eq. (1)) and can be used to describe risk more comprehensively and consistently, where $\Phi[\bullet]$ represents the standard normal cumulative distribution function.

$$\lambda = \int_0^{+\infty} \Phi\left[\frac{\ln s - \eta}{\beta}\right] |dH(s)| \tag{1}$$

Figure 1 illustrates the typical form of these seismic fragility functions, where the magnitude of both η and β vary between limit state and intensity measure (IM), with β describing the uncertainty. This uncertainty can arise from several sources, which are broadly grouped as aleatory and epistemic (Kiureghian and Ditlevsen 2009). Aleatory uncertainty in the context discussed herein typically relates to the inherent uncertainty in the structural response due to the ground motion record variability, which will be the primary source addressed in this study. Other epistemic sources such as capacity models, modelling parameter assumptions in addition to the numerical modelling strategy adopted may also be considered to further increase the overall uncertainty. The choice of IM is an important aspect in the seismic risk assessment. One facet that is typically desirable from any IM is for it to be efficient (Luco and Cornell 2007), meaning that it should be a relatively accurate predictor (i.e. low β) of the structural response and subsequently the overall performance.

This study focusses on the relative efficiency of different IMs for the seismic risk assessment of bridge structures. It first reviews the ways in which IMs are defined for structures such as buildings and how past research has focussed on ensuring certain properties when identifying optimal IMs for their seismic risk assessment. The specific case of bridge structures is then evaluated within this context and it will be seen how some of the building-specific IM findings may not be immediately extendable to multi-modal structures like bridges. Several past approaches to identifying IMs for bridge structures will then be addressed and it will be seen that many studies still rely on non-optimal IM definitions like peak ground acceleration (PGA) and spectral acceleration at a fixed period (HAZUS 2003) in regional risk assessment. This is despite some authors acknowledging that while IMs such as PGA are not ideal, it is the least common denominator and is adopted mainly for convenience. To this end, recent research findings for buildings will be investigated for individual bridges and bridge groups to identify a more efficient and optimal IM based on a simple averaging of spectral accelerations in a pertinent range of periods that has, to the author's knowledge, yet to be tested in this context. The paper uses numerous IM definitions as part of a case study on several bridge structures to evaluate their relative performance for accurate structural performance prediction and risk quantification. The chosen IMs include structure-specific IMs defined using the modal properties of each bridge structure, as well as generic IMs intended to be used to assess groups of structures as part of a larger regional analysis.

2 Assessment of bridge structures

2.1 Intensity measure choice

As illustrated by Bradley (2012a) and others, an IM is the single interface variable that connects seismological and engineering aspects in seismic design and assessment. Seismologists use PSHA to evaluate the probability of exceeding an IML at a specific site over a given period of time. Engineers use this IM to examine the structural response and

evaluate seismic performance knowing the IM's exceedance rate. This characterisation of the interface IM between seismology and engineering, amongst other reasons, intends to avoid relating the structural response to seismological parameters such as magnitude and distance and condensing all pertinent information in the chosen IM for engineering analysis, rendering them sufficient.

Past research on the topic (Kazantzi and Vamvatsikos 2015; Kohrangi et al. 2016a, 2016b; O'Reilly et al. 2018) notes that a desirable IM ought to be efficient, sufficient and for its hazard to be readily computable. The focus of this study is on the second point relating to IM efficiency, which describes the predictive power of the IM, meaning the structural response should exhibit relatively low dispersion for the parameters of interest. Ideally, this dispersion should be as low as possible but still within the bounds of practical implementation. When estimating risk, the predictability of the IM's hazard via PSHA also becomes a factor. The situation may arise where a very efficient predictor of structural response has been identified but which also has a very large ground motion prediction uncertainty. For each IM investigated in this article, ground motion prediction uncertainties are expected to be of a similar order of magnitude, as illustrated by O'Reilly and Monteiro (2019), for example, and also demonstrated to be lower in the case of the average spectral acceleration IMs by Kohrangi et al. (2017a) when compared to any single spectral acceleration based IM. These reductions in dispersions at the various stages of risk assessment may give more refined estimates of risk as a result and will also increase the fidelity in the fragility functions for a given number of ground motion records.

Finally regarding sufficiency, the sufficiency of the results with respect to rupture parameters and record scaling is briefly discussed and checked in Sect. 6.3. Regarding hazard computability, the free availability of the tools used in this study is deemed to be a demonstration of the suitability of all IMs considered here.

2.2 Considerations for bridge structures

Evaluating the dynamic response of a structure naturally leads IMs to be defined in terms of the modal properties, usually the first mode spectral acceleration, $Sa(T_1)$, for buildings dominated by first mode response. In the case of bridges with several spans, there does not tend to be a dominant mode of transverse response (i.e. a mode of response where most of the mass is participating) when monolithic connections to piers of irregular height are utilised, as is the case in this study. This therefore makes the task of choosing a single period to characterise the structural response in terms of $Sa(T)$, which denotes the spectral acceleration at a period T, more difficult. It is noted that bridge structures supported on bearings on piers of regular height will tend to have more regular and dominant modes. To illustrate this, Fig. 2a shows the cumulative distribution of modal mass across each modal period for 7 bridge structures encountered later in Sect. 3. From Fig. 2a, there is generally not any single mode that characterises the dynamic response of bridges, especially when compared to the RC frame structures shown in Fig. 2b, for example. The large initial jump in cumulative modal mass in that case is indicative of the classic first mode dominant response typically observed in buildings. Furthermore, when assessing large numbers of bridges as part of a regional or portfolio assessment, it is almost certain that bridges will possess different vibration periods, making the choice of IM to best suit all structures in the portfolio even more critical. A shrewdly-selected period may be efficient for some bridges but not for

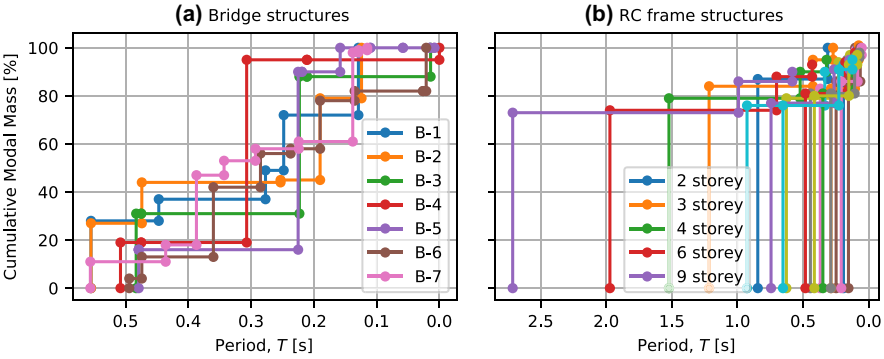

Fig. 2 Illustration of the cumulative modal mass of bridge and RC frame structures studied in O'Reilly and Sullivan (2018) versus vibration period, where several building typologies and heights are plotted and are grouped here in terms of their storey number

others, possibly resulting in increased dispersion and reduced IM efficiency as will be seen in later sections.

2.3 Past and current approaches to intensity measure selection

Improved IMs for bridge structures has been the focus of a relatively limited body of research compared to buildings. Considering the previous points on difficulties in selecting a suitable IM for bridge structures, it is worth looking at what past work has used for these specific typologies. Past studies Borzi et al. (2015), Lupoi et al. (2006), Gardoni et al. (2002), Padgett et al. (2008), Monteiro et al. (2019), Mangalathu et al. (2017a), Cardone et al. (2011), Miano et al. (2016) have examined ways in which fragility functions can be developed and typically adopt PGA as the IM, although $Sa(T)$ has also been utilised (Gardoni et al. 2002; Mangalathu et al. 2017a). Gardoni et al. (2002), for instance, used a systematic model selection for bridge structures and identified spectral acceleration as the most informative IM when constructing probabilistic seismic demand models for Californian bridge bents, with Huang et (2010) also looking at a vector of both $Sa(T)$ and PGV to provide seismic fragility estimates for RC highway bridges in the US, although neither study extended their findings to seismic risk evaluation (i.e. integration with the seismic hazard as per Eq. (1)). For example, Borzi et al. (2015) discussed the development of fragility functions for Italian bridges and noted that while PGA was not an optimal IM for any bridge, it was chosen as the simplest common denominator for the analysis. Miano et al. (2016) also utilised PGA when performing loss assessment of bridge portfolios in Southern Italy. Furthermore, when analysing data from the 1994 Northridge earthquake in the US, Basöz et al. (1999) utilised PGA to aggregate the data and develop fragility functions. Another study by Banerjee and Shinozuka (2008) used PGA as the IM when analysing fragility functions for concrete bridges that can be calibrated with empirical fragility curves constructed based on data from the same earthquake. This was also seen in Elnashai et al. (2004), where when comparing empirically derived fragility functions with data from past events in Northridge and the 1995 Japanese earthquake in Hyogo-ken Nanbu, PGA was employed. Although a simple and convenient solution, PGA response has been shown Padgett et al. (2008) to be a fair performer for bridges when compared to other types of IMs, therefore still has some merit as a response predictor. Some studies have examined

the efficiency of IMs such as PGA and $Sa(T)$ mentioned above, in addition to others like PGV, Arias Intensity, and significant duration, for example. A study by Mehdizadeh et al. (2017) focussed on the potential bias in results due to record scaling when using different IMs such as PGA, PGV, $Sa(T_1)$ along with a relatively novel IM called average spectral displacement intensity (SDI). They noted that the bias was a function of the IM used, with PGA noted for its susceptibility, and that SDI was a much better predictor of response than other IMs based on initial properties like $Sa(T_1)$.

Overall, it can be noted from the above that while PGA is known to be an inefficient IM for bridge structures, it still persists among many past and recent studies. In fact, PGA still tends to be a more favourable solution among some guidelines (MIT 2020) although HAZUS (2003) recommends the use of Sa(1 s) for bridges in the US; however, The general finding is that structural period related spectral quantities like $Sa(T)$ are generally not as efficient as they are in buildings. Velocity-based IMs like PGV have been demonstrated (Monteiro et al. 2019) to generally be the more efficient predictors of extensive damage.

Further to the more classical IM definitions based on ground motion spectral ordinates, other proposals have been made for seismic assessment. Of note is the generalised conditional intensity measure (GCIM) approach (Bradley 2010, 2012b) whereby record selection and hazard consistency can be ensured across a range of IMs and not just limited to spectral quantities. Such an approach is particularly advantageous in situations where duration effects are germane, as in the case of liquefaction (Millen et al. 2020), for example. While the GCIM offers much flexibility, it remains a general approach to record selection to be followed rather than a specific IM recommendation. Ground motion records selected to match a target multivariate conditional distribution of several IMs that are hazard-consistent within this GCIM framework should be trialled and compared with other existing work in the future. Average spectral acceleration, *AvgSa*, Kazantzi and Vamvatsikos (2015), Eads et al. (2015), Cordova et al. (2000), Vamvatsikos and Cornell (2005) and Bianchini et al. (2009) is another prominent candidate to use in seismic assessment. It is defined by Eq. (2) as the geometric mean of N-number spectral accelerations within a user-specified range $[T_{\text{lower}}, T_{\text{upper}}]$. It works on the basis of defining a period range of interest over which the hazard is conditioned, instead of a specific period of vibration. This way, the precise value of a structure's period(s) is not required (as for $Sa(T_1)$) but rather a range in which they are likely to fall.

$$AvgSa = \left[\prod_{i=1}^{N} Sa\left(T_i\right)\right]^{1/N} \quad \text{for } T \in [T_{lower}, T_{upper}] \tag{2}$$

This IM has been examined in several past studies for the collapse assessment of buildings (Eads et al. 2015, 2016, 2013; Dávalos and Miranda 2019a) and has typically linked its definition to the first mode period of vibration. It was noted by Eads et al. (2015), for example, that when compared to $Sa(T_1)$ and computed using an appropriate period range, *AvgSa* showed itself to be a much more efficient collapse predictor and gave more stable predictions of collapse risk in buildings. In particular, they noted the added benefit of including spectral acceleration values both higher and lower than T_1 in the IM definition. For bridge structures, where there is usually no dominant mode of vibration, the use of a period range makes more sense since the entire response usually cannot be adequately linked to a single mode of vibration (Fig. 2). Hence, a direct extension of this past work on buildings that relied on knowing a building's dominant period T_1 to bridge structures is not forgone. In addition, this work aforementioned work focussed solely on the collapse

performance of buildings, where in the case of bridges, other limit states linked to serviceability and continued functionality is also of interest. To date, there has been no extensive study to the author's knowledge examining the performance and potential benefits to be gained by using *AvgSa* as an IM when analysing bridges compared to existing approaches like PGA and *Sa*(*T*), which will be the main focus of this study.

This IM differs to the SDI examined in Mehdizadeh et al. (2017), which computed a spectral intensity over a period range rather than an average, whilst also employing spectral displacement as opposed to spectral acceleration. Also, the authors noted SDI requires tools to be developed that would make its hazard computation feasible and would facilitate the computation of risk, which is discussed later in Sect. 6.6. *AvgSa,* on the other hand, has recently been implemented in the OpenQuake hazard engine (GEM 2019; Kohrangi et al. 2017a) describe a means with which to select ground motion records for the IM. Furthermore, Kohrangi et al. (2017b) demonstrated how multiple sites may be considered in record selection when using *AvgSa*. They showed that for multiple structures in different locations, a single set of ground motion records may be selected based on *AvgSa* (i.e. single set, multiple site/structure) and still maintain many of the benefits typically expected when performing both structure and site-specific record selection and analysis (i.e. multiple set, multiple site/structure). Such a development has a clear application for bridge structures. Furthermore, O'Reilly (2021) has recently shown how *AvgSa* is generally much more efficient and is not prone to biased response predictions for infilled RC structures when compared to other IMs like *PGA*, *PGV* and $Sa(T_1)$. *AvgSa* is therefore investigated alongside the previous IMs examined in the literature.

Mangalathu et al. (2017b) recently examined the bridge classification grouping used by HAZUS when constructing fragility functions for Californian box-girder type bridges with *Sa*(1 s) as the IM. They noted how improvements could be made in the fragility analysis with respect to HAZUS by extending the bridge parameters considered for the classification via various techniques. It will be seen later that the goal of this work is somewhat similar, where instead conventional IMs used in the regional assessment of bridges will be examined and shown how further considerations with other IMs can provide more accurate predictions and contribute to an overall improvement of risk estimation.

3 Case study structures

3.1 Overview

To investigate the impact of using different IMs in the fragility assessment of bridges, 7 multi-span bridges consisting of either 4 or 8 spans of 50 m previously examined by Pinho et al. (2009) and representative of the European context were utilised. The bridge pier sections were RC sections designed according to Eurocode 8 (CEN. Eurocode 8 2005) with a hollow rectangular configuration and the deck was a continuous deck, with reinforcing details illustrated in Fig. 3. Bridge pier heights were either 7 m, 14 m or 21 m and bridges were described as being regular or irregular depending on the variation sequence of pier heights along the structure length. Details are given in Table 1 and illustrated in Fig. 4. Longitudinal reinforcement comprised diameter 20 mm bars placed as shown in Fig. 3, where the bars were evenly spaced at 110 mm in the shorter direction and at 310 mm in the longer direction, with the innermost bars spaced at 600 mm. Concrete cover thickness was 20 mm and the reinforcement had a yield tensile strength of 500 MPa and the concrete

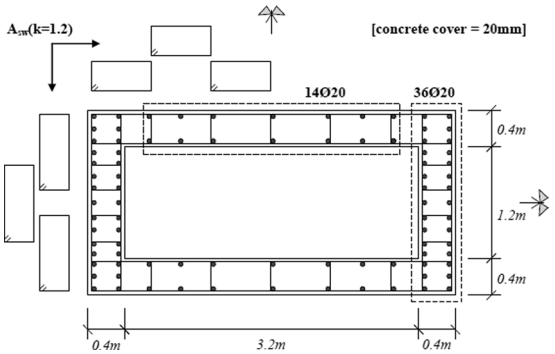

Fig. 3 Details of the cross section utilised for each bridge pier (Pinho et al. 2009), where the shorter side of the section is placed in the direction of the bridge deck

Table 1 Description of case study structure configurations and modal properties

ID	Type	T_1 [s]	T_2 [s]	T_3 [s]	$\%M_1$	$\%M_2$	$\%M_3$	$\Sigma\%M$
B-1	Irregular	0.555	0.447	0.277	28	9	12	49
B-2	Irregular	0.555	0.474	0.253	27	17	1	45
B-3	Regular	0.483	0.475	0.223	31	0	57	88
B-4	Regular	0.508	0.475	0.307	19	0	76	95
B-5	Regular	0.479	0.479	0.225	16	0	74	90
B-6	Irregular	0.494	0.474	0.360	4	9	29	42
B-7	Irregular	0.556	0.436	0.387	11	7	29	47

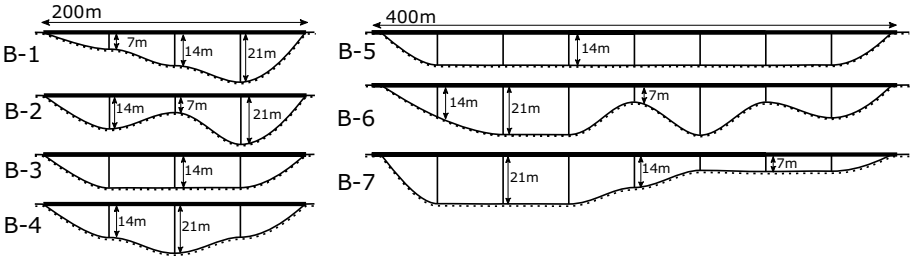

Fig. 4 Illustration of the longitudinal profile of the case study bridge structures considered

compressive strength was 42 MPa. As described in Pinho et al. (2009), the piers were fixed at their base and rigidly connected to the underside of the deck system. The deck ends were placed on linear bearings at the abutments on either side. It was envisaged that by using bridges of varying span number and pier height, and therefore distributions of bridge pier stiffness, the impacts of (1) period elongation due to damage in the pier elements; and (2) contributions from the numerous pertinent modes of response present in bridge structures (Fig. 2), could be examined and their efficiency in response characterisation be quantified.

3.2 Numerical modelling and limit state definition

A numerical model of each bridge was built using OpenSees (McKenna et al. 2010) and is described in detail in O'Reilly and Monteiro (2019). The deck system was modelled using a continuous elastic beam-column element with effective cross section properties and continuous mass. The piers were assumed to be fixed at the base for simplicity and the deck ends were supported upon pot bearings. A more detailed consideration of the foundation could have been considered but this was not anticipated to impact the results presented later on the relative efficiency of different IMs for a multi-modal structural system such a multi-span bridge structure. Pier elements were modelled using lumped plasticity elements, whose parameters were established from moment–curvature analysis and subsequently modelled with a bilinear force–displacement response. To simulate the rupture of the reinforcing bars and subsequent loss of strength in the pier sections, the MinMax criterion available in OpenSees was used to simulate its loss of strength when a certain strain threshold was surpassed. This rupture strain was taken as 0.10 based on the values given in Priestley et al. (1996) for reinforcement steel used in bridges in Europe. Since the main of the study is to analyse the dispersion in response due to record-to-record variability and how it varies amount different IMs, epistemic uncertainties associated with numerical modelling parameters were not considered as part of this study and a single deterministic model was used for each bridge structure. The variability of these modelling parameters and their impacts on the resulting fragility functions could be considered in future studies using methods such as those outlined in Gardoni et al. (2002), for example.

Modal analysis was carried out to identify the dynamic properties of each bridge structure. Table 1 lists the periods, T, and modal masses, M, for the first three modes of vibration along with their sum in each structure corresponding to the transverse direction of response alone. It can be seen that some of the periods tend to be closely spaced and none of the modes comprise a majority of the modal mass, as shown in Fig. 2a. This underlines how, unlike building structures, there tends not to be a predominant mode of response that well represents the entire bridge dynamic response. It is also worth noting how the first three modes of the regular bridge structures comprise most of the mass ($>88\%$), whereas for the irregular cases there is an overall poor representation of modal mass in the first three modes ($<49\%$).

To characterise the structural response with increasing intensity, a structural demand parameter, or engineering demand parameter (EDP), was needed. In bridges, the lack of a dominant mode or an obvious critical element in the structure makes the identification of a suitable EDP a non-trivial task. Global EDPs, such as peak deck displacement, may be used but these do not necessarily differentiate the degree of damage in piers of different height. Piers were noted to be the critical elements characterising the structural damage of the bridges due to their structural configuration. They were modelled as fixed at their base and rigidly connected to the underside of the continuous bridge deck, meaning that largest inelastic demand was observed at their base due to the relative fixity at either end. Considering this and the relative simplicity of the bridge models analysed, element-oriented EDPs were sought here. Monteiro et al. (2019) followed the work of Nielson (2005) and HAZUS (2003) by utilising the maximum displacement-based ductility of all piers as their EDP. A similar approach was adopted here and the peak transient curvature at the base of the piers was monitored during ground shaking to obtain the peak pier section curvature. The maximum value among all bridge piers, φ_{max}, (Fig. 5) was then utilised as the EDP.

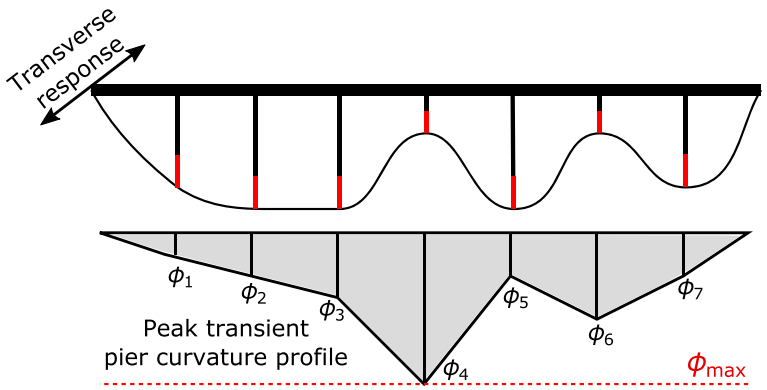

Fig. 5 Definition of the EDP used in the dynamic analysis

To describe the structural performance, two limit states were identified, corresponding to pier section yielding and the peak strength, beyond which the section begins to lose its capacity due to rupturing of the reinforcement bars. The yield curvature was computed using the formulation of Priestley et al. (2007) and checked during moment–curvature analysis, and for peak strength, the section curvature was computed via the reinforcement rupture strain limit. Both limit state definitions are element specific and independent of pier height and therefore a single set of thresholds was used throughout. These two limit states—termed *yielding* and *peak strength* herein—correspond to 1.25mrad and 26.9mrad, respectively. These limit states were based on the flexural response of the pier members, since they were capacity designed using EC8. Other mechanisms such a pier shear failure, unseating of the deck and foundation and abutment failure could also be considered in more detailed and specific studies. For example, Borzi et al. (2015) demonstrated how these could be considered for older bridges in Italy, with possible shear failure and deck unseating observed in past events. These limit states were then collectively considered into a global demand-capacity envelope EDP, as described by Jalayer et al. (2007).

4 Intensity measures

To characterise the evolution of structural damage, an IM was required. Since the purpose of this study was to evaluate the relative IM efficiency, several IMs were considered based on past studies. These were selected based on the most commonly adopted IMs found in the literature in addition to other recently developed IMs that may prove useful for bridge structures. The following IMs were thus considered:

- *PGA*—defined as the peak ground acceleration;
- $Sa(T_1)$—5%-damped spectral acceleration at the first mode period, T_1, of a given structure;
- $Sa(T_{med})$—5%-damped spectral acceleration at the median period, T_{med}, of the first three modes, T_1—T_3, for the structures listed in Table 1;
- $Sa(T)$—5%-damped spectral acceleration at periods, T, equal to 0.3 s, 0.5 s, 1 s, and 2 s;
- *PGV*—defined as the peak ground velocity;

- $AvgSa_{\text{single}}$—average spectral acceleration defined by Eq. (2) in a range of T_{lower} and T_{upper} for each structure;
- $AvgSa_{\text{group}}$—average spectral acceleration defined by Eq. (2) in a range of T_{lower} and T_{upper} for all structures.

A total of 26 IMs were considered, comprising 8 generic group IM definitions (i.e. PGA, PGV, $Sa(T_{\text{med}})$, Sa(0.3 s), Sa(0.5 s), Sa(1 s), Sa(2 s) and $AvgSa_{\text{group}}$) and 14 structure-specific IM definitions (i.e. seven $Sa(T_1)$ and seven $AvgSa_{\text{single}}$), although this was further reduced to 15 considering the overlap in periods shown in Table 2. In the case of PGA and PGV, these quantities are self-explanatory and are simply defined as the absolute peak of the ground acceleration and ground velocity, meaning that they were not in any way connected to a structure's dynamic properties. On the other hand, $Sa(T_1)$ and $Sa(T_{\text{med}})$ correspond to the spectral accelerations at specified periods of the individual structures or the median of the group, meaning that some period information was required for their definition. $Sa(T_1)$ was included due to its relevance in non-linear static procedures and the development of fragility functions via such approaches - e.g. (Perdomo et al. 2020) - whereas Sa(1 s) was included because of its recommendation in the HAZUS guidelines in the US. Other fixed definitions of $Sa(T)$ were included to investigate the efficiency of IMs defined in a similar manner to HAZUS. For these IMs, the information in Table 1 was utilised and Table 2 describes the IM definition for each bridge.

For $AvgSa$, a period range [T_{lower}, T_{upper}] with a spacing of 0.1 s was defined using the modal properties listed in Table 1, as per Eq. (2). Two interpretations of this IM were considered: (1) $AvgSa_{\text{single}}$; and (2) $AvgSa_{\text{group}}$, where $AvgSa_{\text{single}}$ was defined using the modal properties of a single bridge structure, whereas $AvgSa_{\text{group}}$ was defined using modal properties of all bridges. This was done to investigate the use of $AvgSa$ as an *IM* for a more portfolio-oriented assessment in addition to a bridge-specific context, which would be extremely advantageous for regional assessment of several bridges should the IM be found to be more efficient than existing approaches in Sect. 6. The period range for $AvgSa_{\text{single}}$ was defined as [$0.5T_3$, $1.5T_1$]. T_{lower} was defined as the third mode period factored down by 0.5 to anticipate other higher modal contributions since the irregular bridge configurations have modes beyond the third contributing notably to the dynamic response. T_{upper} was taken as T_1 amplified by 1.5 to account for the effects of period elongation during non-linear response. This rationale in establishing period ranges based on modal properties and anticipated non-linear behaviour is similar to what has been investigated for buildings in the past also Kazantzi and Vamvatsikos (2015) and Eads and Miranda (2013). For the

Table 2 Period information used to define each of the candidate IMs

ID	$Sa(T_1)$	$Sa(T_{\text{med}})$	$AvgSa_{\text{single}}$		$AvgSa_{\text{group}}$	
	T_1	T_{med}	T_{lower}	T_{upper}	T_{lower}	T_{upper}
B-1	0.56	0.47	0.14	0.83	0.11	0.83
B-2	0.56		0.13	0.83		
B-3	0.48		0.11	0.72		
B-4	0.51		0.15	0.76		
B-5	0.48		0.11	0.72		
B-6	0.49		0.18	0.74		
B-7	0.56		0.19	0.83		

definition of $AvgSa_{\text{group}}$, T_{lower} was determined as 0.5 times the 16th percentile of the T_3 values, $T_{3,16\%}$, whereas T_{upper} was determined as 1.5 times the 84th percentile of the T_1 values, $T_{1,84\%}$. The lower limit is suggested as the 16th percentile value for bridge structures in order to cover the majority of the higher mode values and not be biased by any outlier period value. Likewise, the upper limit was established using the 84th percentile to cover the majority of the first mode periods in a given bridge portfolio. It is worth noting that these period ranges do not necessarily need to be based on actual modal data but just need to cover the relevant period range for those structures.

5 Hazard analysis and ground motion selection

5.1 Site description and hazard analysis

A site in L'Aquila, Italy with a V_{s30} of 300 m/s was chosen. Site hazard curves (Fig. 6) were quantified for each IM and the causal rupture characteristics (e.g. magnitude and distance etc.) contributing most to each IM's mean hazard curve were identified. The OpenQuake engine (GEM 2019) was used to perform PSHA calculations with the SHARE source model (Woessner et al. 2015) for the site considered. The ground motion prediction equations (GMPEs) from Boore and Atkinson (2008) were used meaning that each IM considered was characterised with GMPEs from the same study.

5.2 Selection of ground motion records

To characterise the structural response with increasing intensity, sets of 40 ground motion records were chosen for each IM. These records were selected for discrete intensity levels in order to carry out multiple stripe analysis (MSA) (Jalayer 2003) on the bridge structures.

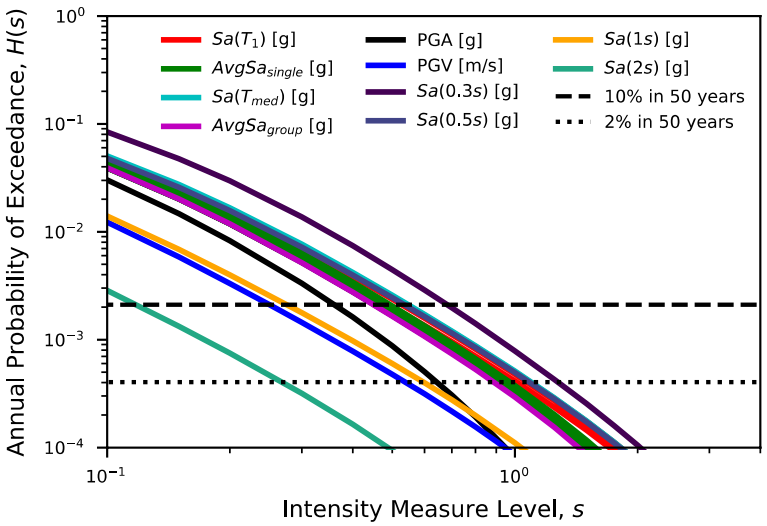

Fig. 6 Illustration of the mean hazard curves identified for a site in L'Aquila, Italy for each IM considered

MSA was chosen over other approaches such as incremental dynamic analysis (Vamvatsikos and Cornell 2002), cloud analysis (Jalayer 2003) or modified cloud analysis (Jalayer et al. 2017) such that the chosen records' seismological characteristics could be matched to the hazard disaggregation information at each of the selected intensity levels. Cloud analysis methods, however, may have the benefit of not requiring ground motion record scaling in certain situations, therefore removing any possible scaling bias in the results obtained; this potential bias will be discussed and checked for in Sect. 6.3 for the MSA results used herein.

A total of 9 intensity levels were investigated, corresponding to probabilities of exceedance ranging from 50 to 0.1% in 50 years, ensuring that the structural response covering initial damage right up to collapse could be characterised. For the $Sa(T)$-based IMs, the conditional spectrum (CS) approach outlined by Baker (2011) was followed, whereas its extension to *AvgSa*-based selection described in Kohrangi et al. (2017a) was followed for those cases. For what concerns the correlations between the spectral ordinates at the different periods of vibration, the model proposed by Baker and Jayaram (2008) was utilised. The hazard consistency of the ground motion record sets selected was also ensured at all periods other than those for which they were selected. Hazard consistency was taken to mean that the rates of exceedance of the selected ground motions' response spectra are consistent with, or match, the site ground motion hazard curves obtained from PSHA at all relevant periods. This was a necessary step to ensure that they do indeed match the site hazard and will theoretically lead to the same estimation of risk (Bradley 2012a; Lin et al. 2013).

For PGA and PGV, CS-based methods were not used and ground motion records with rupture characteristics consistent with the mean PSHA disaggregation information at each intensity level were chosen. This was done in order to replicate record selection typically adopted for such IMs in past years, where conditional hazard approaches were generally not considered and ground motions could be matched to code spectra (Lupoi et al. 2006), synthetically generated (Padgett et al. 2008), or both (Elnashai et al. 2004), for example. Other more advanced methods of record selection such as the GCIM approach could have been adopted, where hazard-consistent records are chosen using a more advanced generalisation of the CS approach. This option was intentionally disregarded here in order to remain consistent with more traditional approaches to selecting ground motions for bridges in the literature. The implications of this choice will be discussed later. Figure 7 shows an example of a ground motion selection for both $Sa(T)$ and *AvgSa*. Ground motion records considered in this study did not consider near-source effects, therefore the findings presented herein require further validation in such scenarios.

6 Results

6.1 MSA results

With the ground motion record set for each IM identified in Sect. 5.1, MSA was carried out using the numerical model for each case study bridge structure. This returned the distribution of bridge response characterised via the EDP described in Fig. 5 versus IML. For example, the MSA results for case study bridge B-3 and different IMs are illustrated in Fig. 8. As shown, the individual response ordinates are marked for each ground motion record at each intensity stripe, corresponding to one of the 9 intensity

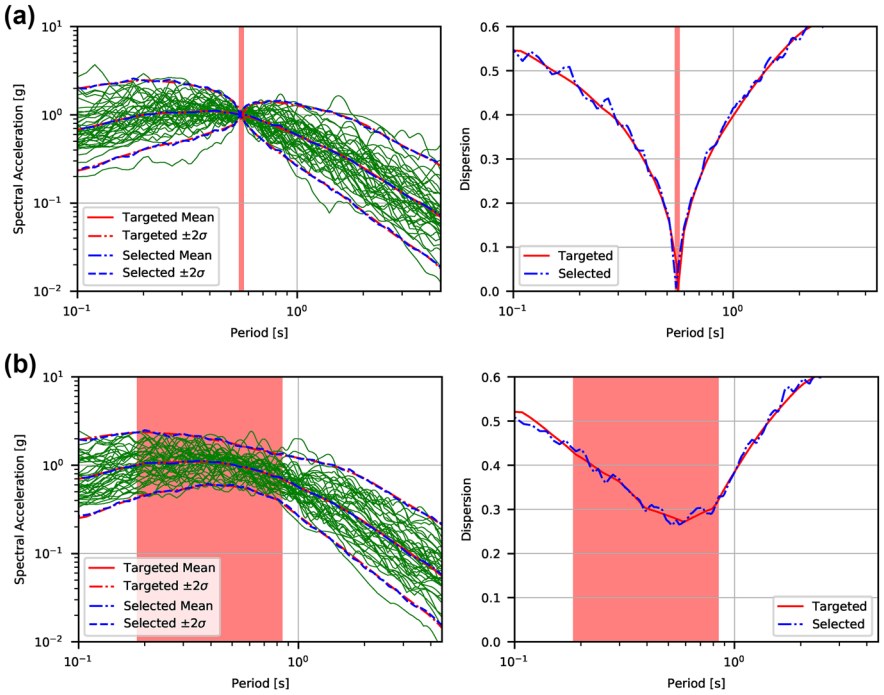

Fig. 7 Set of 40 ground motion records selected for the B-7 structure at the 2% probability of exceedance in 50 years for (top) $Sa(T=0.56$ s) and (bottom) $AvgSa$, where matching of the selected mean and dispersion is compared to the targeted distribution. The red shaded zones indicate the conditioning period value or range used

levels investigated. The median values are also plotted to illustrate the trend of increased bridge response with respect to increased shaking intensity. It is also possible to note the increased dispersion of points with increasing IML and also between IMs. Additionally, the data at each intensity stripe was evaluated using the Kolmogorov–Smirnov goodness of fit test at the 5% significance level (Benjamin and Cornell 1970), showing the assumption of lognormality to be satisfactory for all bridges and IMs investigated. From a total of 630 cases (i.e. 7 bridges, 10 IMs, 9 IMLs), the null hypothesis that the data follows a lognormal distribution was rejected in just 9 (1.4%) instances.

6.2 Fragility functions

To examine the efficiency in assessing the response of the case study structures, several evaluations were examined. First, the efficiency of each IM in quantifying the structural response was evaluated from both a demand-based and an intensity-based perspective. That is, the dispersion in the IMLs required to exceed a given EDP due to record-to-record variability, $\beta_{\mathrm{IML|EDP}}$, (demand-based) and the dispersion in response for a given IML, $\beta_{\mathrm{EDP|IML}}$, (intensity-based) were evaluated. Demand-based evaluation describes the distribution of IMLs required to result in a given level of structural demand being exceeded, whereas the

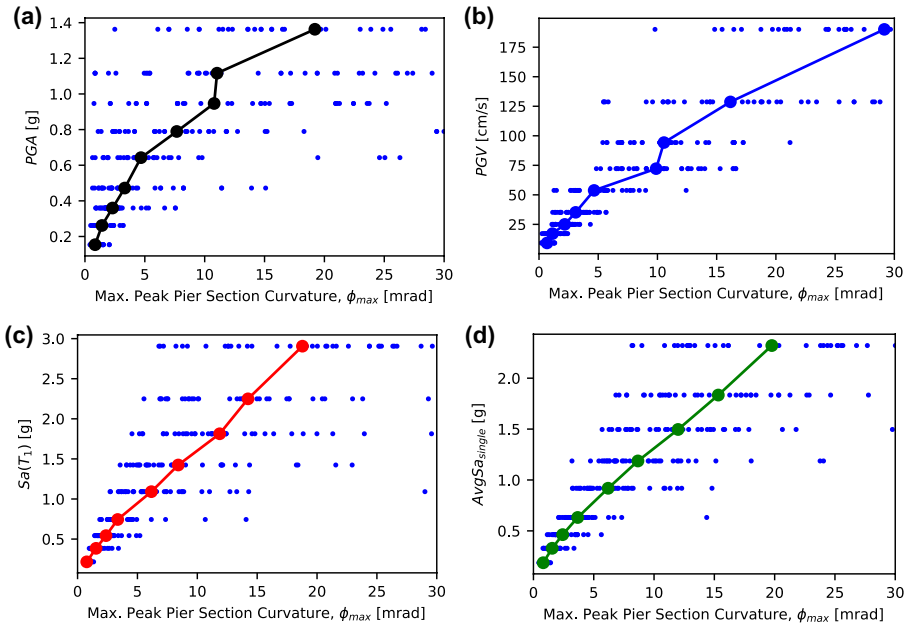

Fig. 8 Illustration of the MSA results obtained for case study bridge B-3 for different IMs

latter is the more classic description of structural response for a given intensity that modern code prescriptions tend to focus on, as discussed by Lin et al. (2013) for example. By integrating the demand-based results with the site mean hazard curves shown in Fig. 6, the annual exceedance rates of the demands (i.e. MAFE) were computed for each IM in a risk-based evaluation. This comparison will highlight the differences between each IM in terms of their ability to quantify the seismic risk associated with each bridge.

Since MSA is set up to return the distribution of EDP for a given IML (i.e. intensity-based), obtaining the distribution of IML for a given EDP required some further data processing. In this study, this distribution was assumed to be lognormal with median, $\eta_{\text{IML|EDP}}$, and dispersion, $\beta_{\text{IML|EDP}}$. To identify these parameters, the maximum likelihood method of fitting (Baker 2015; Iervolino 2017) was used, whereby the fraction of EDP exceedances at each IML was used to fit a suitable continuous lognormal distribution, which then characterise the fragility functions shown in Fig. 9. Care was taken in the selection of the return period range to examine (Sect. 5.2) to ensure that an adequate number of exceedances were observed at all EDP levels examined such that fragility functions could be fitted. Figure 9 shows the fragility functions derived following this approach for the two limit states considered, with Table 3 listing their associated distribution parameters. Each of these fragility functions fitted was tested for lognormality using the Kolmogorov–Smirnov goodness of fit test at the 5% significance level. For each structure, IM, limit state and EDP value evaluated, the conditions to deduce a lognormal distribution were met.

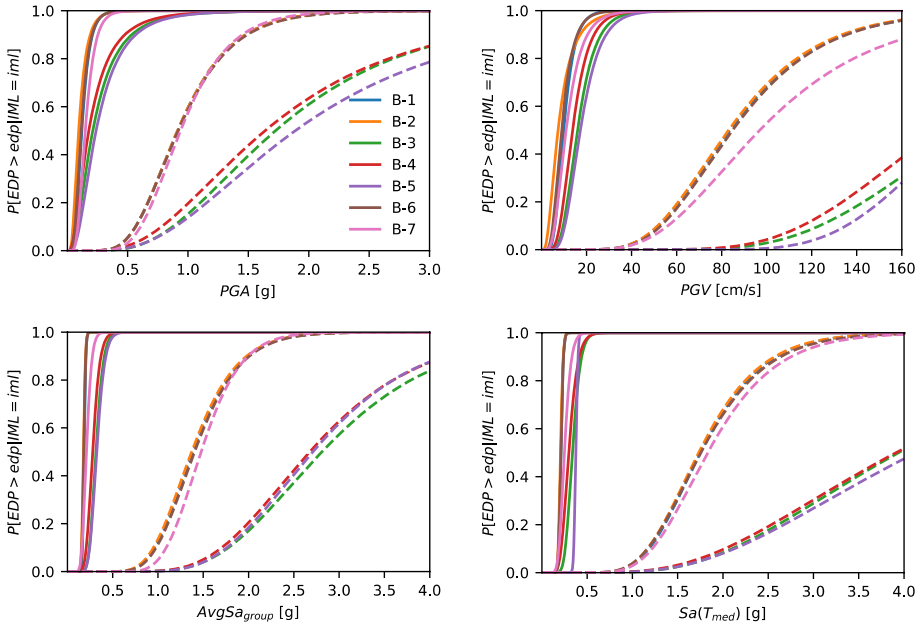

Fig. 9 Fragility functions fitted using MSA data for each bridge, where the solid and dashed lines denote the yielding and peak strength limit states, respectively

Table 3 Fragility function parameters for each bridge, with the pairs of values representing the median and dispersion ($\eta_{\text{IML|EDP}}/\beta_{\text{IML|EDP}}$) for both limit states, respectively

ID	Yielding				Peak Strength			
	PGA	*PGV*	$AvgSa_{\text{group}}$	$Sa(T_{\text{med}})$	*PGA*	*PGV*	$AvgSa_{\text{group}}$	$Sa(T_{\text{med}})$
B-1	0.12/0.43	9.8/0.39	0.19/0.08	0.21/0.10	0.91/0.37	83.6/0.37	1.39/0.28	1.75/0.30
B-2	0.10/0.54	7.3/0.67	0.18/0.10	0.21/0.11	0.92/0.37	83.1/0.37	1.37/0.29	1.73/0.31
B-3	0.21/0.72	15.9/0.40	0.32/0.20	0.34/0.21	1.72/0.53	189.5/0.33	2.81/0.36	3.94/0.49
B-4	0.18/0.77	13.8/0.41	0.28/0.23	0.30/0.26	1.64/0.58	176.1/0.33	2.68/0.35	3.91/0.52
B-5	0.24/0.67	17.2/0.40	0.32/0.21	0.38/0.05	1.89/0.58	184.0 /0.24	2.71/0.33	4.13/0.52
B-6	0.12/0.46	8.9/0.45	0.18/0.10	0.21/0.10	0.92/0.38	84.9/0.37	1.40/0.28	1.76/0.32
B-7	0.15/0.41	10.9/0.49	0.21/0.21	0.25/0.22	0.94/0.34	96.9/0.43	1.48/0.24	1.83/0.32

6.3 Sufficiency of results

As previously mentioned, the discussion and comparison of IMs in terms of their predictive power or dispersion rests on the assumption that the analysis results are sufficient and it is a computable IM to estimate via hazard analysis. Sufficiency implies that the results obtained for each IM are not biased by rupture or other parameters associated with the ground motion records used. This section presents a brief check of this to ensure the sufficiency of all results and permit further discussion in the following sections.

Figure 10 shows a plot of the relative sufficiency versus the rupture parameters magnitude, M, Joyner-Boore distance, R_{jb}, and level of scaling employed for each record. It plots the residuals of the results, ε, defined as the ratio of each individual response value normalised by the median value at the respective intensity. This way, any trend or bias in results with respect to the median values arising from a dependence on these parameters (i.e. lack of sufficiency) will become apparent from the plots. The relative sufficiency is judged here graphically in order to compare the IMs collectively. Other approaches, such as checking for statistical significance via p-values - e.g. (Eads et al. 2015) - may also be used but simplified relative sufficiency, as described by Dávalos and Miranda (2019b, 2020), is also a simple and effective way to evaluate and compare IMs. As seen from Fig. 10, all of the results obtained for each IM show little to no dependence on neither the source rupture parameters of the ground motions nor to the level of scaling used to match them to the hazard during selection. This is evident from the near horizontal slope of the trendline for each IM, illustrating that while certain residuals may have been large for some individual records, these were not as a result of some other overall property of the ground motions biasing the results. It is noted, however, that the IMs Sa(1 s) and Sa(2 s) were seen to be a little dependent on R_{jb} compared to other IMs examined, as shown in Fig. 10b. Also worth noting is the similarity of the lines between IMs, indicating that there were no other notable differences in IM relative sufficiency. Therefore, it may be concluded from Fig. 10 that the IMs examined in this study for these case study bridges are generally sufficient for seismic risk assessment.

6.4 Demand-based evaluation

Figure 11 shows the mean $\beta_{IM|EDP}$ due to record-to-record variability for each IM examined for all bridge structures. What is immediately obvious is that at yielding, PGA and PGV, in addition to Sa(1 s) and Sa(2 s), are inefficient predictors of bridge response due to their relatively large dispersion compared to other IMs. At peak strength, when the bridge structures underwent some non-linear response, pier damage, and period elongation, Fig. 11 shows how the mean dispersion of these same IMs reduced but remained relatively high. For the $Sa(T)$-based IMs, the mean dispersion was quite low at yielding but increased past PGA and PGV at peak strength in some cases. Notable exceptions were Sa(1 s) and Sa(2 s) which were relatively poor at yielding, but increased in their mean efficiency at peak strength. This is especially the case for Sa(1 s), which is recalled to be the IM recommended by HAZUS. Velocity-based IMs were also highlighted in past studies (O'Reilly and Monteiro 2019; Monteiro et al. 2019) to be relatively good predictors of bridge response at ultimate limit states but rather poor at serviceability limit states. Based on the mean results shown in Fig. 11, there does not appear to be any great benefit in using a $Sa(T)$-based IM over PGA or PGV for the assessment of bridge structures at their ultimate limit state based just on dispersion, which gives some further support to the past use of this IM. *AvgSa*-based IMs, on the other hand, showed quite a good performance at both limit states. The mean *AvgSa*-based dispersion in Fig. 11 was relatively low at the yielding limit state, although just slightly above the lowest $Sa(T)$-based IMs, and was generally lower at the peak strength limit state compared to other IMs.

Figure 12 further demonstrates these observations by plotting $\beta_{IM|EDP}$ versus demand, φ_{max}. For most bridges, PGV, PGA, Sa(1 s) and Sa(2 s) had high dispersion at low demands and decreased slightly with increasing demand. The other $Sa(T)$-based IMs, on the other

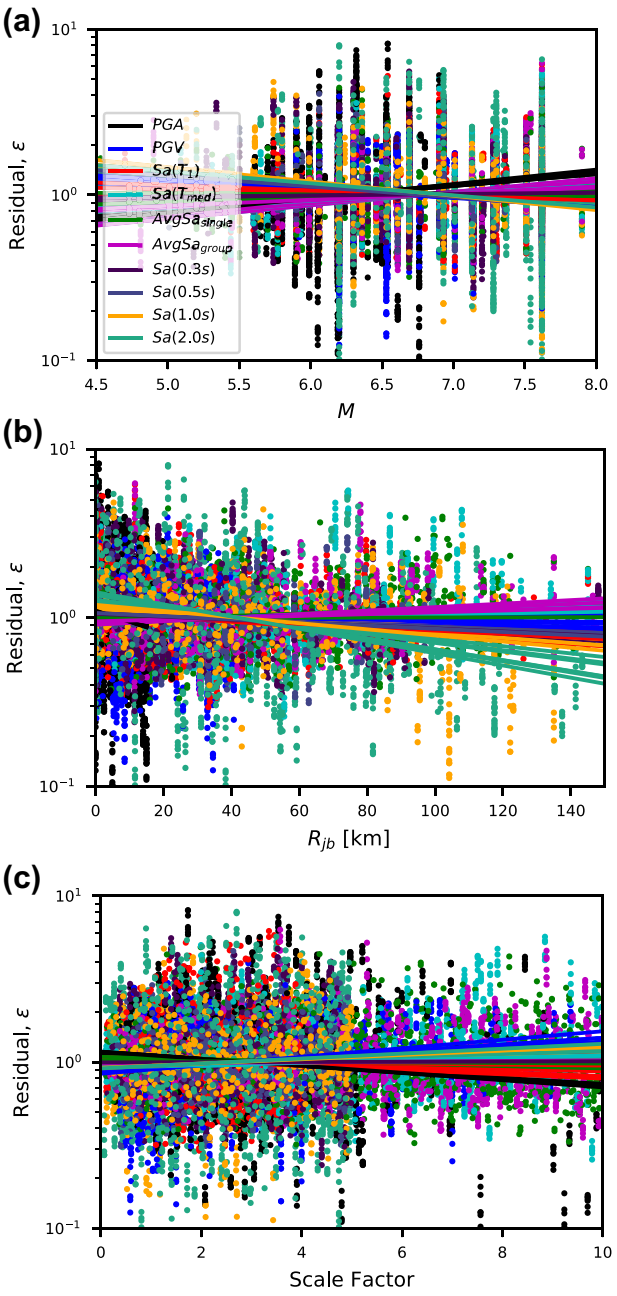

Fig. 10 Relative sufficiency of each bridge and IM results' residuals with respect to rupture parameters and ground motion scaling factors, illustrating the results for each ground motion record from each bridge and IM pair alongside the observed trend

hand, generally got progressively worse with increased demand for most cases, whereas *Sa*(1 s) and *Sa*(2 s) improved. What is interesting to note is that the *AvgSa*-based IMs were generally quite stable across all levels of demand. Both the single and group *AvgSa* IMs remained relatively consistent, whereas other IMs' dispersion either increased or reduced. This can make the choice of IM trickier depending on which limit states are of immediate

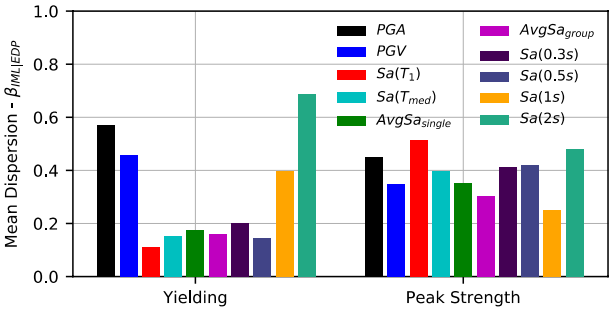

Fig. 11 Mean dispersion for case study bridges at the yielding and peak strength limit states

interest, as from Fig. 12 alone, it may seem wise to use $Sa(T_1)$ for assessing serviceability limit states and PGV or Sa(1 s) to assess ultimate limit states since they had the lowest dispersions. *AvgSa* in this case, however, removes the need for such a choice. This is also seen for B-6 shown in Fig. 12e, for example, where each IM's dispersion tended to gradually increase, with PGV making a notable drop but the *AvgSa*-based IMs retaining a desirably low dispersion. From a demand-based perspective, the *AvgSa*-based IMs were the best performers for the case study bridges examined here across all limit states. It is also worth highlighting that there was no difference in dispersion between the structure-specific $AvgSa_{\text{single}}$ and the group-based definition $AvgSa_{\text{group}}$, meaning that analysts may develop fragility functions for many bridges using the same set of *AvgSa*-based ground motions and, based on the present findings, could expect a similar level of predictive efficiency had they used structure-specific IMs and individually tailored ground motion sets. This would have clear benefits for a regional assessment-oriented problem such as bridge structures. It would also have the benefit of allowing the comparison of fragility functions for different structures directly via their common IM. This type of comparison may be useful to convey the relative strength capacity of different structures within a bridge portfolio in a simple manner.

6.5 Intensity-based evaluation

In addition to examining the dispersion in intensities for a given level of demand exceedance ($\beta_{\text{IM|EDP}}$), the dispersion in demand at a given intensity, $\beta_{\text{EDP|IM}}$, was also examined to provide further insight into each IM's predictive power. While not as of much use from a risk evaluation perspective compared to the demand-based results, intensity-based evaluation is still quite a common prescription in design codes, as discussed by Lin et al. (2013). Therefore, the ability to more accurately quantify the response of a bridge structure for a given return period of seismic shaking is also of interest. In addition, intensity-based evaluation forms the basis of the structural analysis input required for loss estimation [e.g. Mackie et al. (2009)]. It is noted that the dispersion in these structural analysis results would also be expected to be influenced greatly by the type of ground motion selection procedure employed at each IML, where using a CS-based approach, as was done here, or a GCIM-based approach could further influence the loss assessment results. As such, care should be taken to ensure the methods adopted are suitable for the analysis aims.

Figure 13 shows the $\beta_{\text{EDP|IM}}$ versus return period, T_{R}, for each IM where it can be seen that response for the PGA and PGV IMs had relatively high dispersion, especially at low intensities. PGV tended to decrease with increasing intensity but PGA showed

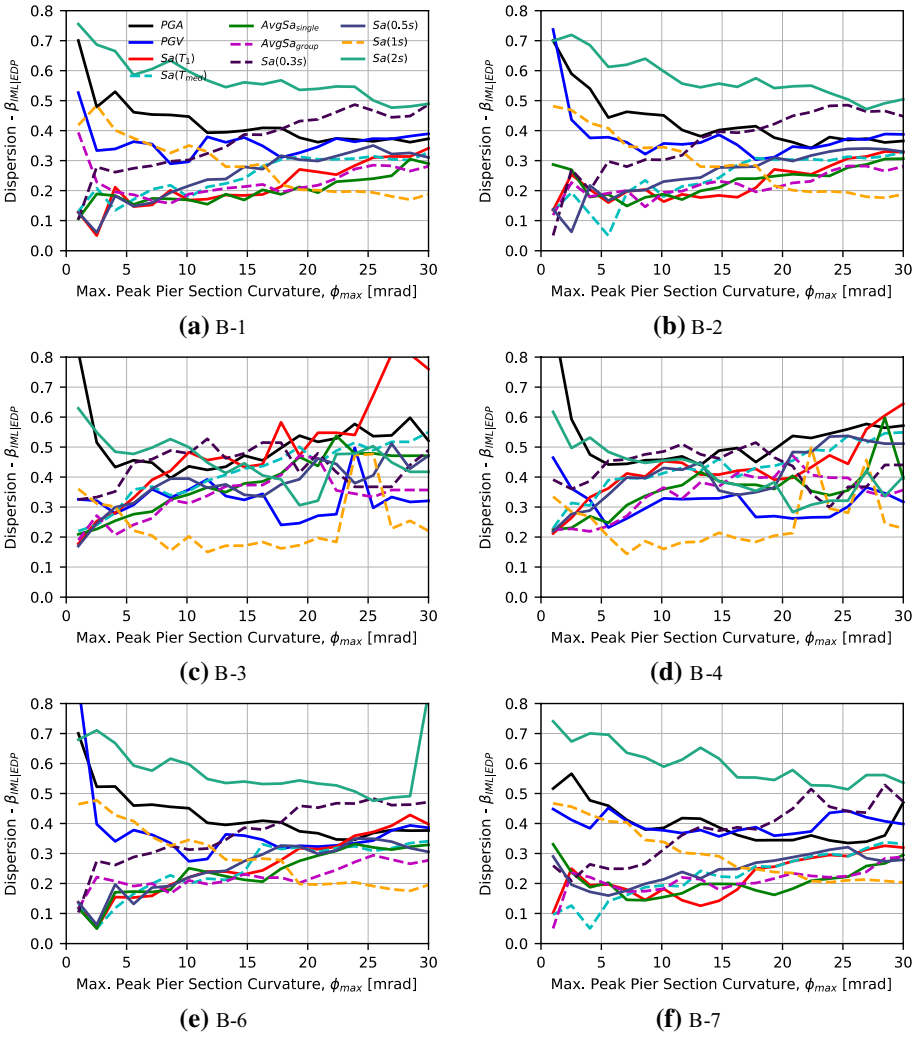

Fig. 12 Dispersion in intensity with respect to demand, $\beta_{\text{IM}|\text{EDP}}$, for case study bridges

an increase in dispersion with increasing T_{R}. The relative similarity in the trends for PGA and PGV among the different bridges was due to the same ground motion sets being used in each case. For the $Sa(T)$ and $AvgSa$ IMs, trends similar to the demand-based dispersion were observed, with a relatively modest level of dispersion maintained throughout. This was especially true for the $AvgSa$-based IMs, whereas the $Sa(T)$-based IMs did not show the same increase as previously observed. Notably, Sa(1 s) increased in efficiency for higher return periods, indicating that it is a valid candidate for characterising response at high levels of ground shaking, whereas Sa(2 s) tended to be a poor predictor throughout; this is to be expected given how far the conditioning period of $T=2$ s is from the modal properties listed in Table 1 for each bridge. Again, there was no discernible difference between results obtained using the structure-specific and group-based definitions of these IMs.

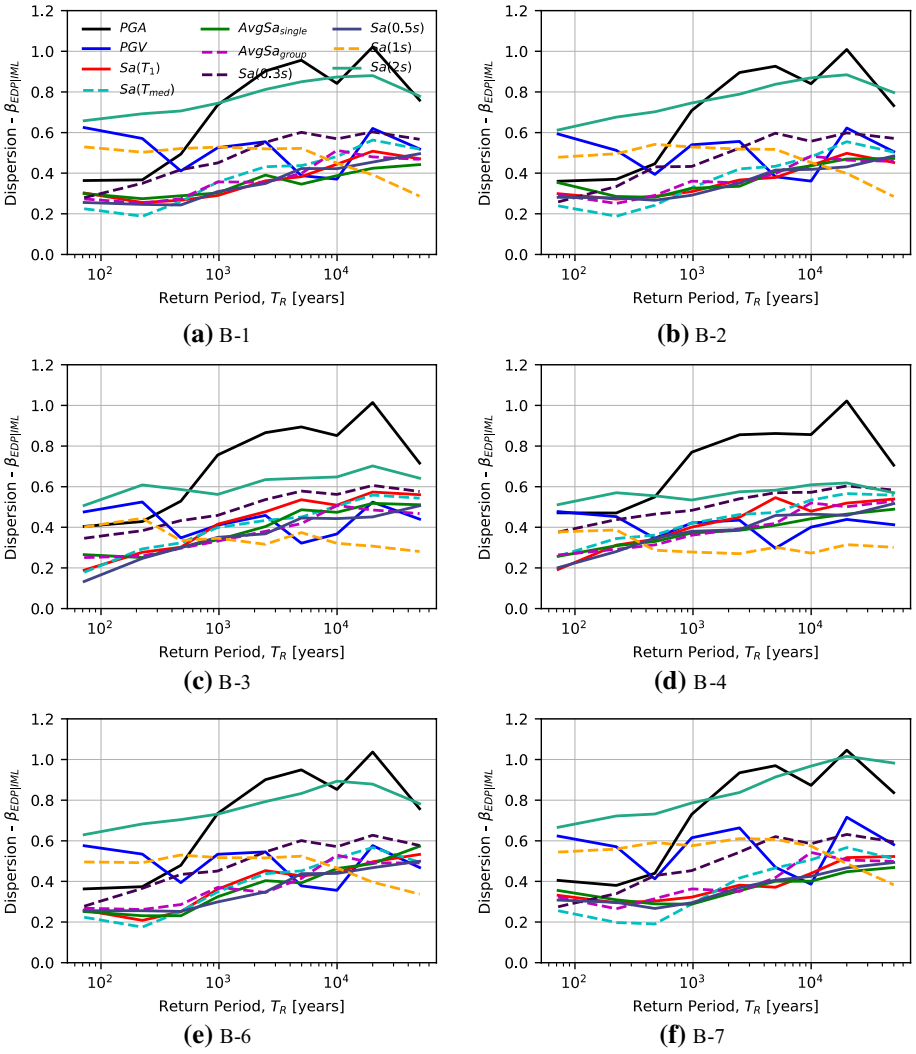

Fig. 13 Dispersion in demand with respect to intensity level, $\beta_{\text{EDP|IML}}$, for case study bridges

Therefore, for a single intensity level of the bridges examined in this study, the dispersion in PGA and PGV results tended to be much higher than any other IM, and were seen here to be quite similar. This would imply that for an analyst looking to verify the performance of a bridge structure at a return period of 475 years, for example, the choice of IM may have an important impact on the results obtained and care should be taken. The relatively large uncertainty in the PGA and PGV results observed here may lead to an inaccurate, or highly disperse, estimation of structural response and possibly affect the decisions made. This uncertainty may be reduced by using a larger set of ground motion records, which has obvious drawbacks with regards to computational efficiency.

6.6 Risk-based evaluation

In the demand-based evaluation, the $\eta_{\text{IML|EDP}}$ and $\beta_{\text{IML|EDP}}$ of the lognormally distributed IMLs required to exceed a given EDP level were characterised for each IM at increasing levels of structural demand. This distribution was then integrated directly here with each IM's mean hazard curve to compute the MAFE of an EDP, λ, as follows:

$$\lambda = \int_0^{+\infty} \Phi\left[\frac{\ln s - \eta_{IML|EDP}}{\beta_{IML|EDP}}\right] |dH(s)| \tag{3}$$

where $\Phi[\bullet]$ is the standard normal cumulative distribution function. Computing the MAFE this way considers record-to-record variability only, but other sources of uncertainty may also be included. Since the mean hazard curves were adopted from the hazard results provided by the OpenQuake engine in Sect. 5, the integration of the seismic fragility functions derived in Sect. 6.2 and integrated as per Eq. (3) provides a mean estimate of the annual exceedance frequency for a given EDP. The uncertainty associated with the hazard curves may also be included to compute the EDP's annual exceedance frequency as described in Cornell et al. (2002) and Vamvatsikos (2013), for example, but is not dealt with here and only MAFE is compared. Directly integrating the fragility functions with the hazard curves shown in Fig. 6 using Eq. (3) gave the demand-exceedance curves of the case study structures for the different IMs shown in Fig. 14.

Before discussing the details of these plots, it is first necessary to state what was being sought and evaluated here. Since there is no feasible way to check or confirm the validity of these risk estimates, some inference must be made. MAFE curves commence at zero demand with a λ corresponding to the baseline hazard, described as the hazard curve value at an infinitesimally small intensity (i.e. $\lim_{s\to 0} H(s)$). MAFE reduces with increased demand and for deformation-based EDPs, λ will gradually approach the structure's mean annual frequency of collapse for very large demand. To evaluate the different IM estimates of λ for intermediate demands, it is typical to look for the consistency between them. The logic behind this interpretation is that while it is not possible to experimentally verify any observed value of λ, a consistency between the different IM observations of λ would strongly indicate that the structure's unique value of seismic risk for that level of demand is indeed the observed value and this can be used as the benchmark with which to judge other IMs' under or overestimation of risk. This stems from the findings of Bradley (2012a), subsequently corroborated by Lin et al. (2013) and others, who demonstrated that the estimates of a risk-based quantity like MAFE is unique for a structure and is independent of the IM choice or $Sa(T)$ conditioning period. This finding is subject to the conditions that: 1) the ground motion records used to quantify the structural response and estimate the MAFE are hazard-consistent, as was the case here; 2) the IM employed be a sufficient, which was also the case here for all IMs examined; and 3) for the IM to be an efficient indicator of the structural response. Therefore, for each of the IMs examined, the MAFEs would be expected to converge to the same value for each bridge. It is noted that such MAFE versus demand, or demand-hazard curves, may be compared and somewhat validated with those derived via extensive physics-based simulations, as discussed by Bradley et al. (2015), for example. However, as noted in that study, this approach would not be feasible for the study outlined here.

In Fig. 14, the MAFE for a given pier section curvature was seen to be relatively similar in terms of trend amongst the IMs. Almost all converged toward the same estimate of λ, with the exception of PGA, PGV and Sa(2 s) that tend to deviate from the others.

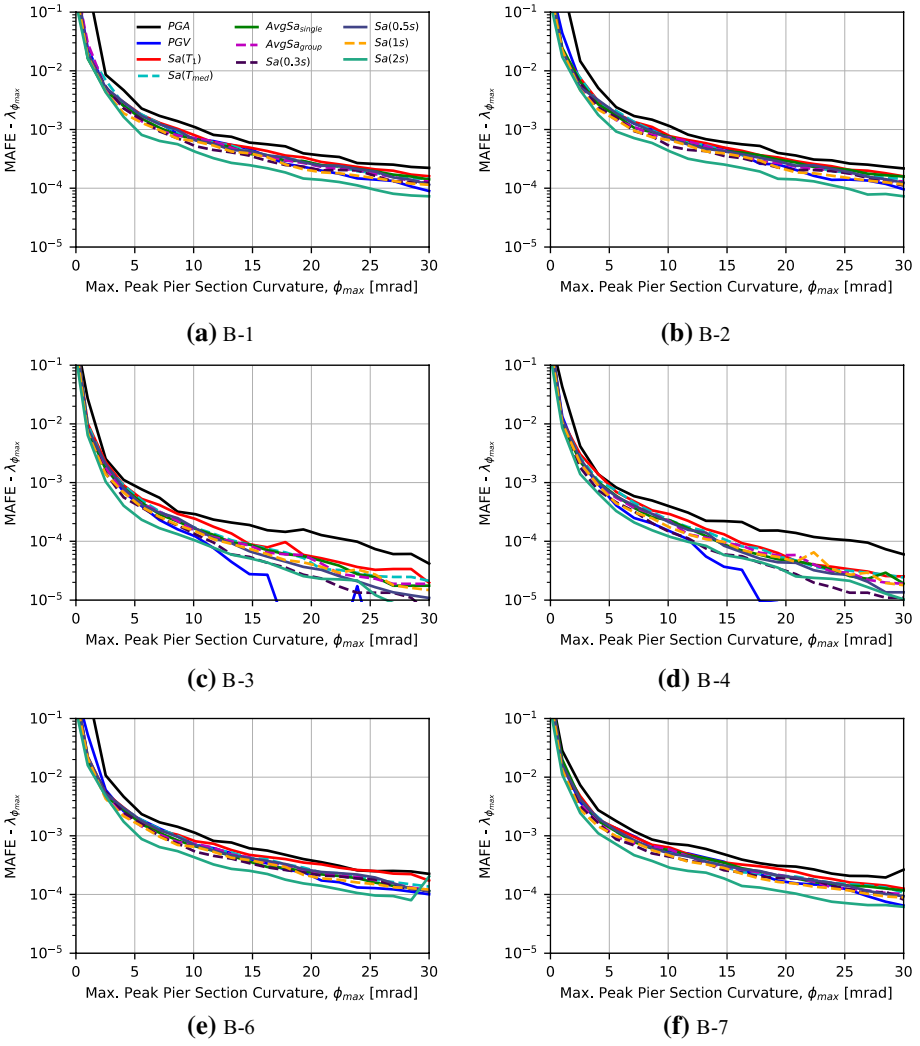

Fig. 14 MAFE with respect to demand for case study bridges

It is noted that for some cases in Fig. 14, slight oscillations were observed locally in the demand-hazard curves. Further inspection showed that these resulted because of the non-monotonicity of the IML-EDP results and the need to bin the MSA data. Increasing the number of IMLs used in the ground motion record selection would alleviate this issue but the relative trend between the demand-hazard curves would not be anticipated to change overall. Furthermore, it can be seen that there was no major difference between using $Sa(T_1)$ or $Sa(T_{\text{med}})$ as they estimated essentially the same risk in each case, although this is also likely due to the close similarity of the IM definitions. Very similar demand-hazard curves were also noted for Sa(0.3 s), Sa(0.5 s) and Sa(1 s), illustrating how their relative efficiency and hazard consistency led to stable estimates of risk throughout. This was not the case for Sa(2 s), however, where its relative inefficiency observed in previous sections meant that it was consistently underestimating with respect to the other $Sa(T)$-based IMs,

despite its hazard-consistent selection. While not apparent from Fig. 14, *Sa*(1 s) tended to exhibit the same underestimation at lower levels of demand, reflection the large dispersion observed earlier. Likewise for the *AvgSa*-based IMs, where the structure-specific and group definitions were very similar for all cases. Therefore, in order to assess the risk of exceeding a certain damage state in a group of bridge structures, an analyst may simply adopt a single IM of either *Sa*(*T*) or $AvgSa_{\text{group}}$ for all structures instead of identifying individual IMs and repeating the ground motion record selection process many times, although care must be taken regarding the conditioning period when using *Sa*(*T*) and also *AvgSa* to a lesser extent.

For PGA and PGV, the results seen here for the bridge structures should not be surprising and were mainly due to the choices made during the ground motion record selection process. This particular approach was followed here to investigate two issues. The first was concerning the choice of IM and its implementation in past studies. The demand-based and intensity-based evaluations in Sects. 6.4 and 6.5 have shown that PGA and PGV are not awful predictors of bridge response, but other IMs tended to be much better for all limit states and not just some. This point should motivate a shift away from these traditional IMs in favour of the more attractive and flexible options explored here. The second point concerns the hazard consistency of the ground motions. To ensure a hazard-consistent selection for PGA and PGV, a CS-based approach may be adopted but would require the appropriate correlation models, similar to how the *Sa*(*T*) and *AvgSa* implementations required the one by Baker and Jayaram (2008) in Sect. 5.2. The more advanced GCIM approach could also have been adopted and would require the same types of correlation models. With either of these two approaches, the same risk-consistent outputs observed in Fig. 14 for all IMs could be expected. In fact, Bradley (2012a) showed this to work well for IMs like PGA, PGV and *Sa*(*T*) on a combined bridge and foundation system's response. This type of detailed selection procedure has typically not been considered in past studies and can perhaps lead to some confusion about whether an IM is suitable or not. Simply looking at the dispersion in results like those presented in Sects. 6.4 and 6.5 may be misleading if the risk-based parameters are not considered. The ground motion records used here for PGA and PGV could be casually described as being hazard-consistent, since they were all conditioned to the exact IML obtained from PSHA at each return period and the source characteristics of each ground motion record were compatible with the hazard disaggregation. However, this description of hazard consistency is not at all the same as the hazard-consistency implied by Bradley (2012a) in his application of PGA or PGV as an IM, or the definition utilised here and stated in Sect. 5.2. Simply stating that the records selected at each hazard level were 'consistent' with the PSHA results and expecting risk estimates to be as good as any other IM may not be enough unless the degree of consistency respects the same conditions originally intended. The GCIM approach to record selection may not always be vital but its implications when making risk-based decisions should not always be taken for granted. The impact of such a relatively casual interpretation for PGA and PGV hazard consistency is evident in Fig. 14 for the bridge structures examined here, whereby PGA tended to overestimate the risk with respect to the other hazard-consistent IMs. PGV tended to underestimate the risk for the bridges and progressively deviated from the other IMs with increased demand in some cases. This strict and thorough compatibility of the selected records across all IMs, and not just the one of interest, is what should ideally be sought in risk studies and the casual approach utilised here should be avoided. The same sort of observations would be expected with ground motion records selected and scaled to match the uniform hazard spectra specified by design codes, which again could be interpreted as a form of hazard consistency. The spectral ordinates at each period will not be

consistent with the conditional spectrum, despite matching the uniform hazard spectrum, as shown in Lin et al. (2013).

7 Summary and Conclusions

This article looked at intensity measures (IM) for the seismic risk assessment of bridge structures characteristic of the European context. Several simple case study bridges with different configuration were modelled and analysed. Their dynamic response with respect to increasing ground shaking intensity was characterised using multiple stripe analysis (MSA) and the exceedance of two limit states corresponding to pier section yielding and peak strength was quantified. Different IMs were considered to evaluate the relative efficiency in structural response prediction of bridges across all pertinent limit states of response. The considered IMs corresponded to those typically adopted in the literature, such as peak ground acceleration (PGA) and peak ground velocity (PGV), spectral acceleration, $Sa(T)$ in addition to a recently introduced IM termed average spectral acceleration, *AvgSa*, which was examined on both a structure-specific and multiple structure basis. Their efficiency was evaluated by examining the demand-based and intensity-based outputs from MSA followed by an evaluation of the seismic risk-exceedance curves of each bridge configuration. Based on the results of this study, the following conclusions can be made:

- From an IM dispersion perspective, PGV and PGA were seen to be reasonable predictors of bridge response at ultimate limit states but less efficient predictors at serviceability limit states;
- $Sa(T)$-based IMs whose conditioning period lay close to the fundamental mode of the bridge response were the best predictors of structural response at serviceability but progressively lost their predictive power towards the ultimate limit states due to period lengthening;
- $Sa(1\text{ s})$, as recommended by HAZUS, showed rather large dispersion at serviceability limit states but improved towards the ultimate limit state. This in contrast to above where the predictive power was lost with increasing demand. $Sa(2\text{ s})$ did not exhibit any such improvement in its generally predictive power, which was noted to result in differences in its risk estimates by consistently underestimating with respect to other hazard-consistent IMs;
- There did not appear to be any advantage gained in terms of reducing dispersion when using $Sa(T)$ over PGA at ultimate limit states;
- *AvgSa* was seen to outperform all other IMs for demand-based evaluations, with a consistently low dispersion observed for all level of demands for all bridges examined;
- There was no discernible loss in predictive power when using the *AvgSa* IM defined for all structures as opposed to the individually tailored *AvgSa* IMs—this presents convenient advantages when considering the assessment of regional portfolios of bridges;
- For intensity-based assessments, PGA and PGV showed a consistently larger dispersion in demands at all intensities compared to other IMs, which may potentially lead to inaccurate structural response verifications at code-defined intensities and possible require larger ground motion record sets for more accurate response quantification;
- All of the $Sa(T)$ and *AvgSa*-based IMs exhibited a consistent level of risk for each bridge structure, corroborating past findings in the literature about a structure's seismic

risk being independent of the IM used to quantify it, so long as the ground motions are hazard-consistent and a suitable IM is used;

- Lastly, and perhaps more importantly for what concerns the scope of this study, the risk results obtained here demonstrated that the use of PGA or PGV, as has been typically adopted in the past for bridge structure assessment, should not be expected to provide accurate estimates of seismic risk when casual approaches to ground motion selection are adopted, in addition to their general inefficiency as an IM compared to others examined here.

To conclude, this study has tackled some issues typically overlooked or taken for granted when assessing groups of bridge structures. It was seen how traditional methods are generally less favourable and can be potentially erroneous in their quantification of seismic risk. It should be noted that the case study examined was limited to 7 case study reinforced concrete bridge structures with monolithic connections between piers and the continuous deck system, which would be expected to be found in Europe. Further studies may be carried out to validate these findings for different bridge typologies, such as those found in the US with different connection details and configuration, as part of future work but the general observation of *AvgSa* providing more accurate predictions would still be anticipated to hold. That said, these methods to quantify risk with readily available tools are therefore recommended for the future development of bridge fragility functions and risk models for regional assessment, as implemented in a recent project examining critical infrastructures in Europe and surrounding areas (O'Reilly et al. 2019).

Acknowledgements The work presented in this paper has been developed within the framework of the project "Dipartimenti di Eccellenza", funded by the Italian Ministry of Education, University and Research at IUSS Pavia. It has also received support from the INFRA-NAT project co-funded by European Commission ECHO—Humanitarian Aid and Civil Protection. Project reference: 78329—INFRA-NAT—UPM-2017-PP-AG. Discussions with Ricardo Monteiro on aspects related to this research and the assistance of Elisa Zuccolo for the hazard analysis implementation in OpenQuake are both gratefully acknowledged.

References

Baker JW (2011) Conditional mean spectrum: tool for ground-motion selection. J Struct Eng 137(3):322–331. https://doi.org/10.1061/(ASCE)ST.1943-541X.0000215

Baker JW (2015) Efficient analytical fragility function fitting using dynamic structural analysis. Earthq Spectra 31(1):579–599. https://doi.org/10.1193/021113EQS025M

Baker JW, Jayaram N (2008) Correlation of spectral acceleration values from NGA ground motion models. Earthq Spectra 24(1):299–317. https://doi.org/10.1193/1.2857544

Banerjee S, Shinozuka M (2008) Mechanistic quantification of RC bridge damage states under earthquake through fragility analysis. Probab Eng Mech 23(1):12–22. https://doi.org/10.1016/j.probengmech.2007.08.001

Basöz NI, Kiremidjian AS, King SA, Law KH (1999) Statistical analysis of bridge damage data from the 1994 Northridge, CA. Earthquake Earthq Spectra 15(1):25–54. https://doi.org/10.1193/1.1586027

Benjamin JR, Cornell CA (1970) Probability. McGraw-Hill Book Company, Statistics and decision for civil engineers

Bianchini M, Diotallevi P, Baker JW (2009) Prediction of inelastic structural response using an average of spectral accelerations. In: ICOSSAR09: 10th International Conference on Structural Safety and Reliability, Osaka, Japan.

Boore DM, Atkinson GM (2008) Ground-Motion prediction equations for the average horizontal component of PGA, PGV, and 5%-damped PSA at spectral periods between 0.01 s and 10.0 s. Earthq Spectra 24(1):99–138. https://doi.org/10.1193/1.2830434

Borzi B, Ceresa P, Franchin P, Noto F, Calvi GM, Pinto PE (2015) Seismic vulnerability of the Italian roadway bridge stock. Earthq Spectra 31(4):2137–2161. https://doi.org/10.1193/070413EQS190M

Bradley BA (2012b) A ground motion selection algorithm based on the generalized conditional intensity measure approach. Soil Dyn Earthq Eng 40:48–61. https://doi.org/10.1016/j.soildyn.2012.04.007

Bradley BA (2012a) The seismic demand hazard and importance of the conditioning intensity measure. Earthquake Eng Struct Dynam 41(11):1417–1437. https://doi.org/10.1002/eqe.2221

Bradley BA (2010) A generalized conditional intensity measure approach and holistic ground-motion selection. Earthq Eng Struct Dynam 39(2):1321–1342. https://doi.org/10.1002/eqe.995

Bradley BA, Burks LS, Baker JW (2015) Ground motion selection for simulation-based seismic hazard and structural reliability assessment. Earthq Eng Struct Dynam 44(13):2321–2340. https://doi.org/10.1002/eqe.2588

Cardone D, Perrone G, Sofia S (2011) A performance-based adaptive methodology for the seismic evaluation of multi-span simply supported deck bridges. Bull Earthq Eng 9(5):1463–1498. https://doi.org/10.1007/s10518-011-9260-8

CEN. Eurocode 8: Design of Structures for Earthquake Resistance-Part 2: Bridges (EN 1998–2:2005). Brussels, Belgium: 2005.

Cordova P, Deierlein GG, Mehanny S, Cornell CA (2000) Development of a two-parameter seismic intensity measure and probabilistic assessment procedure. In: Proceedings of the 2nd US–Japan Workshop on Performance-based Earth- quake Engineering Methodology for RC Building Structures, Sapporo, Hokkaido, Japan

Cornell CA, Krawinkler H (2000) Progress and challenges in seismic performance assessment. PEER Center News 3(2):1–2

Cornell CA, Jalayer F, Hamburger RO, Foutch DA (2002) Probabilistic basis for 2000 SAC federal emergency management agency steel moment frame guidelines. J Struct Eng 128(4):526–533. https://doi.org/10.1061/(ASCE)0733-9445(2002)128:4(526)

Dávalos H, Miranda E (2019a) Evaluation of the scaling factor bias influence on the probability of collapse using Sa(T1 as the Intensity Measure. Earthq Spectra 35(2):679–702. https://doi.org/10.1193/011018EQS007M

Dávalos H, Miranda E (2019b) Filtered incremental velocity: a novel approach in intensity measures for seismic collapse estimation. Earthq Eng Struct Dynam 48(12):1384–1405. https://doi.org/10.1002/eqe.3205

Dávalos H, Miranda E (2020) Evaluation of FIV3 as an intensity measure for collapse estimation of moment-resisting frame buildings. J Struct Eng 146(10):04020204. https://doi.org/10.1061/(ASCE)ST.1943-541X.0002781

Der Kiureghian A, Ditlevsen O (2009) Aleatory or epistemic? Does it matter? Struct Saf 31(2):105–112. https://doi.org/10.1016/j.strusafe.2008.06.020

Eads L, Miranda E (2013) Seismic collapse risk assessment of buildings: effects of intensity measure selection and computational approach. Blume Report No 184 2013.

Eads L, Miranda E, Krawinkler H, Lignos DG (2013) An efficient method for estimating the collapse risk of structures in seismic regions. Earthq Eng Struct Dynam 42(1):25–41. https://doi.org/10.1002/eqe.2191

Eads L, Miranda E, Lignos DG (2015) Average spectral acceleration as an intensity measure for collapse risk assessment. Earthq Eng Struct Dynam 44(12):2057–2073. https://doi.org/10.1002/eqe.2575

Eads L, Miranda E, Lignos D (2016) Spectral shape metrics and structural collapse potential. Earthq Eng Struct Dynam 45(10):1643–1659. https://doi.org/10.1002/eqe.2739

Elnashai AS, Borzi B, Vlachos S (2004) Deformation-based vulnerability functions for RC bridges. Struct Eng Mech 17(2):215–244. https://doi.org/10.12989/sem.2004.17.2.215

Gardoni P, Der Kiureghian A, Mosalam KM (2002) Probabilistic capacity models and fragility estimates for reinforced concrete columns based on experimental observations. J Eng Mech 128(10):1024–1038. https://doi.org/10.1061/(ASCE)0733-9399(2002)128:10(1024)

Gardoni P, Mosalam KM (2003) Kiureghian A der (2003) Probabilistic seismic demand models and fragility estimates for RC bridges. J Earthq Eng 7(sup001):79–106. https://doi.org/10.1080/13632460309350474

GEM (2019) The OpenQuake engine user instruction manual: 189. https://doi.org/10.13117/GEM.OPENQUAKE.MAN.ENGINE.3.7.1.

HAZUS (2003) Multi-hazard loss estimation methodology-earthquake model. Washington, DC, USA

Huang Q, Gardoni P, Hurlebaus S (2010) Probabilistic seismic demand models and fragility estimates for reinforced concrete highway bridges with one single-column bent. J Eng Mech 136(11):1340–1353. https://doi.org/10.1061/(ASCE)EM.1943-7889.0000186

Iervolino I (2017) Assessing uncertainty in estimation of seismic response for PBEE. Earthq Eng Struct Dynam 46(10):1711–1723. https://doi.org/10.1002/eqe.2883
Jalayer F (2003) Direct probabilistic seismic analysis: implementing non-linear dynamic assessments. PhD Thesis, Stanford University, USA
Jalayer F, Franchin P, Pinto PE (2007) A scalar damage measure for seismic reliability analysis of RC frames. Earthq Eng Struct Dynam 36(13):2059–2079. https://doi.org/10.1002/eqe.704
Jalayer F, Ebrahimian H, Miano A, Manfredi G, Sezen H (2017) Analytical fragility assessment using unscaled ground motion records. Earthq Eng Struct Dynam 46(15):2639–2663. https://doi.org/10.1002/eqe.2922
Kazantzi AK, Vamvatsikos D (2015) Intensity measure selection for vulnerability studies of building classes. Earthquake Eng Struct Dynam 44(15):2677–2694. https://doi.org/10.1002/eqe.2603
Kilanitis I, Sextos A (2019) Integrated seismic risk and resilience assessment of roadway networks in earthquake prone areas. Bull Earthq Eng 17(1):181–210. https://doi.org/10.1007/s10518-018-0457-y
Kohrangi M, Vamvatsikos D, Bazzurro P (2016a) Implications of intensity measure selection for seismic loss assessment of 3-D Buildings. Earthq Spectra 32(4):2167–2189. https://doi.org/10.1193/112215EQS177M
Kohrangi M, Bazzurro P, Vamvatsikos D (2016b) Vector and scalar IMs in structural response estimation: part II-building demand assessment. Earthq Spectra 32(3):1525–1543. https://doi.org/10.1193/053115EQS081M
Kohrangi M, Bazzurro P, Vamvatsikos D, Spillatura A (2017a) Conditional spectrum-based ground motion record selection using average spectral acceleration. Earthq Eng Struct Dynam 46(10):1667–1685. https://doi.org/10.1002/eqe.2876
Kohrangi M, Vamvatsikos D, Bazzurro P (2017b) Site dependence and record selection schemes for building fragility and regional loss assessment. Earthq Eng Struct Dynam 46(10):1625–1643. https://doi.org/10.1002/eqe.2873
Lin T, Haselton CB, Baker JW (2013) Conditional spectrum-based ground motion selection. Part I: Hazard consistency for risk-based assessments. Earthq Eng Struct Dyn 42(12):1847–1865. https://doi.org/10.1002/eqe.2301
Lin T, Haselton CB, Baker JW (2013) Conditional spectrum-based ground motion selection. Part II: Intensity-based assessments and evaluation of alternative target spectra. Earthq Eng Struct Dyn 42(12):1867–1884. https://doi.org/10.1002/eqe.2303
Luco N, Cornell CA (2007) Structure-specific scalar intensity measures for near-source and ordinary earthquake ground motions. Earthq Spectra 23(2):357–392. https://doi.org/10.1193/1.2723158
Lupoi G, Franchin P, Lupoi A, Pinto PE (2006) Seismic fragility analysis of structural systems. J Eng Mech 132(4):385–395. https://doi.org/10.1061/(ASCE)0733-9399(2006)132:4(385)
Mackie KR, Wong JM, Stojadinović B, (2009) Post-earthquake bridge repair cost and repair time estimation methodology. Earthq Eng Struct Dyn 39:281–301. https://doi.org/10.1002/eqe.942
Mangalathu S, Jeon JS, Padgett JE, DesRoches R (2017a) Performance-based grouping methods of bridge classes for regional seismic risk assessment: application of ANOVA, ANCOVA, and non-parametric approaches. Earthq Eng Struct Dynam. https://doi.org/10.1002/eqe.2919
Mangalathu S, Soleimani F, Jeon JS (2017b) Bridge classes for regional seismic risk assessment: Improving HAZUS models. Eng Struct 148:755–766. https://doi.org/10.1016/j.engstruct.2017.07.019
McKenna F, Scott MH, Fenves GL (2010) Nonlinear finite-element analysis software architecture using object composition. J Comput Civ Eng 24(1):95–107. https://doi.org/10.1061/(ASCE)CP.1943-5487.0000002
Mehdizadeh M, Mackie KR, Nielson BG (2017) Scaling bias and record selection for quantifying seismic structural demand. J Struct Eng 143(9):04017117. https://doi.org/10.1061/(ASCE)ST.1943-541X.0001855
Miano A, Jalayer F, De Risi R, Prota A, Manfredi G (2016) Model updating and seismic loss assessment for a portfolio of bridges. Bull Earthq Eng 14(3):699–719. https://doi.org/10.1007/s10518-015-9850-y
Millen MDL, Rios S, Quintero J, Viana da Fonseca A (2020) Prediction of time of liquefaction using kinetic and strain energy. Soil Dyn Earthq Eng. https://doi.org/10.1016/j.soildyn.2019.105898
MIT (2020) Linea guida per la classificazione e gestione del rischio, la valutazione della sicurezza, ed il monotoraggio dei ponti esistenti
Monteiro R, Zelaschi C, Silva A, Pinho R (2019) Derivation of fragility functions for seismic assessment of rc bridge portfolios using different intensity measures. J Earthq Eng 23(10):1678–1694. https://doi.org/10.1080/13632469.2017.1387188
Nielson BG (2005) Analytical fragility curves for highway bridges in moderate seismic zones. Georgia Institute of Technology, USA

O'Reilly GJ (2021) Limitations of Sa(T1) as an intensity measure when assessing non-ductile infilled RC frame structures. Bull Earthq Eng 19(6):2389–2417. https://doi.org/10.1007/s10518-021-01071-7

O'Reilly GJ, Monteiro R (2019) On the efficient risk assessment of bridge structures. In: COMPDYN 2019-7th international conference on computational methods in structural dynamics and earthquake engineering, Crete Island, Greece. https://doi.org/10.7712/120119.6933.18933.

O'Reilly GJ, Kohrangi M, Bazzurro P, Monteiro R (2018) Intensity measures for the collapse assessment of infilled RC frames. In: 16th European conference on earthquake engineering, Thessaloniki, Greece.

O'Reilly GJ, Sullivan TJ (2018) Probabilistic seismic assessment and retrofit considerations for Italian RC frame buildings. Bull Earthq Eng 16(3):1447–1485. https://doi.org/10.1007/s10518-017-0257-9

O'Reilly GJ, Abarca A, Monteiro R, Borzi B, Calvi GM (2019) Towards regional safety assessment of bridge infrastructure. In: ICASP13-13th international conference on applications of statistics and probability in Civil Engineering, Seoul, South Korea: 2019. https://doi.org/10.22725/ICASP13.377.

Padgett JE, Nielson BG, DesRoches R (2008) Selection of optimal intensity measures in probabilistic seismic demand models of highway bridge portfolios. Earthq Eng Struct Dynam 37(5):711–725. https://doi.org/10.1002/eqe.782

Perdomo C, Monteiro R, Sucuoğlu H (2020) Development of fragility curves for single-column RC Italian bridges using nonlinear static analysis. J Earthq Eng. https://doi.org/10.1080/13632469.2020.1760153

Pinho R, Monteiro R, Casarotti C, Delgado R (2009) Assessment of continuous span bridges through nonlinear static procedures. Earthq Spectra 25(1):143–159. https://doi.org/10.1193/1.3050449

Priestley MJN, Seible F, Calvi GM (1996) Seismic Design and Retrofit of Bridges. Wiley, New York

Priestley MJN, Calvi GM, Kowalsky MJ (2007) Displacement-based seismic design of structures. IUSS Press, Pavia, Italy

Vamvatsikos D (2013) Derivation of new SAC/FEMA performance evaluation solutions with second-order hazard approximation. Earthq Eng Struct Dynam 42(8):1171–1188. https://doi.org/10.1002/eqe.2265

Vamvatsikos D, Cornell CA (2002) Incremental dynamic analysis. Earthq Eng Struct Dynam 31(3):491–514. https://doi.org/10.1002/eqe.141

Vamvatsikos D, Cornell CA (2005) Developing efficient scalar and vector intensity measures for IDA capacity estimation by incorporating elastic spectral shape information. Earthq Eng Struct Dynam 34(13):1573–1600. https://doi.org/10.1002/eqe.496

Woessner J, Laurentiu D, Giardini D, Crowley H, Cotton F, Grünthal G et al (2015) The 2013 European Seismic Hazard Model: key components and results. Bull Earthq Eng 13(12):3553–3596. https://doi.org/10.1007/s10518-015-9795-1